

A real-time thermal field theoretical analysis of Kubo-type Shear viscosity : Numerical understanding with simple examples

Sabyasachi Ghosh

¹Instituto de Fisica Teorica, Universidade Estadual Paulista, Rua Dr. Bento Teobaldo Ferraz, 271, 01140-070 Sao Paulo, SP, Brazil

Abstract

A real-time thermal field theoretical calculation of shear viscosity has been described in the Kubo formalism for bosonic and fermionic medium. The two point function of viscous stress tensor in the lowest order provides one-loop skeleton diagram of boson or fermion field for bosonic or fermionic matter. According to the traditional diagrammatic technique of transport coefficients, the finite thermal width of boson or fermion is introduced in their internal lines during the evaluation of boson-boson or fermion-fermion loop diagram. These thermal widths of ϕ boson and ψ fermion are respectively obtained from the imaginary part of self-energy for $\phi\Phi$ and $\psi\Phi$ loops, where interactions of higher mass Φ boson with ϕ and ψ are governed by the simple $\phi\phi\Phi$ and $\bar{\psi}\psi\Phi$ interaction Lagrangian densities. A two-loop diagram, having same power of coupling constant as in the one-loop diagram, is deduced and its contribution appears much lower than the one-loop values of shear viscosity. Therefore the one-loop results of Kubo-type shear viscosity may be considered as leading order results for this simple $\phi\phi\Phi$ and $\bar{\psi}\psi\Phi$ interactions. This approximation is valid for any values of coupling constant and at the temperatures greater than the mass of constituent particles of the medium.

1 Introduction

A medium can be perturbed slightly away from its equilibrium state due to quantum fluctuations at finite temperature. The responses to these fluctuations can be determined from the dissipative quantities of the medium. The different fluxes originating from their corresponding thermodynamical forces can appear in the medium to restore the system to its equilibrium state. The transport coefficients like shear and bulk viscosities are proportional constants of the linear relations between these fluxes and forces.

With the help of Kubo formula, the transport coefficients can be microscopically estimated from their corresponding retarded thermal correlators in the low frequency limit. For example, the shear viscosity coefficient can be obtained from the retarded correlator of the viscous stress tensor. The simplest possible anatomical representation of the correlator is a one-loop kind of diagram, where a finite thermal width has to be included in the propagator of the constituent particle. This is a very well established technique [1, 2, 3, 4, 5, 6, 7], which is generally adopted to get a non-divergent value of the transport coefficient. Beyond the one-loop, there will be infinite class of planar ladder diagrams, which have the same power of coupling constant as in the one-loop diagram. The reason is that the additional coupling constants from the interaction vertices of any higher order diagram are exactly cancelled by the additional thermal widths coming from the each loop of that diagram. For this purpose, different ways of re-summed technique are proposed for ϕ^4 theory [8, 9, 10, 11], as well as for hot QCD [12]. In this context, a Kubo-type shear viscosity calculation for medium with ϕ boson or ψ fermion has been derived in a generalized manner where

a simple $\phi\phi\Phi$ or $\psi\psi\Phi$ interaction Lagrangian is considered. The Φ boson is assumed as a higher mass intermediate particle, which is supposed to be appeared in the elastic $\phi\phi$ or $\psi\psi$ scattering. We can take $\pi\pi\sigma$ [13] or $QQ\pi$ [14] interaction as a practical example of such a case.

At first, the simplest possible diagrammatic representation of shear viscosity as a $\phi\phi$ or $\psi\psi$ loop is derived explicitly in the real-time thermal field theory (RTF), which is addressed in Sec. (2). For getting a non-divergent shear viscosity, a finite thermal width of ϕ or ψ has to be introduced owing to the traditional diagrammatic calculation of transport coefficient. In Sec. (3), the thermal width of ϕ or ψ is deduced from the imaginary part of its thermal self-energy for $\phi\Phi$ or $\psi\Phi$ loop. The possibilities of different infinite number of diagrams for the $\phi\phi\Phi$ interaction are pointed out in Sec. (4), where a two-loop diagram is explicitly derived in RTF. During numerical estimations of one-loop and two-loop contributions in shear viscosity, two-loop is substantially suppressed due to presence of additional number of thermal distribution functions appearing in the multiplicative way. These numerical results are discussed in Sec. (5), and Sec. (6) concludes the article.

2 Formalism

From the simple derivation of Kubo formula [15, 16], we are starting our calculation with the expression of shear viscosity in momentum space [3],

$$\eta = \frac{1}{20} \lim_{q_0, \vec{q} \rightarrow 0} \frac{A_\eta(q_0, \vec{q})}{q_0}, \quad (1)$$

where

$$A_\eta(q_0, \vec{q}) = \int d^4x e^{iq \cdot x} \langle [\pi_{ij}(x), \pi^{ij}(0)] \rangle_\beta \quad (2)$$

is spectral function of space component of the viscous-stress tensor, $\pi^{\mu\nu}$ and $\langle \hat{O} \rangle_\beta$ for any operator \hat{O} denotes the equilibrium ensemble average,

$$\begin{aligned} \langle \hat{O} \rangle_\beta &= \text{Tr} \frac{e^{-\beta H} \hat{O}}{Z} \\ \text{with } Z &= \text{Tr} e^{-\beta H}. \end{aligned} \quad (3)$$

The $\pi^{\mu\nu}$ comes from the dissipative part of total energy-momentum tensor, $T^{\mu\nu}$. In the relativistic dissipative hydrodynamics [17, 18] the $T^{\mu\nu}$ can be decomposed into an ideal part $T_0^{\mu\nu}$ and a dissipative part $T_D^{\mu\nu}$.

$$i.e. \quad T^{\mu\nu} = T_0^{\mu\nu} + T_D^{\mu\nu}, \quad (4)$$

where

$$\begin{aligned} T_0^{\mu\nu} &= \epsilon u^\mu u^\nu - P \Delta^{\mu\nu} \\ \text{and } T_D^{\mu\nu} &= K^\mu u^\nu + K^\nu u^\mu - \pi^{\mu\nu}, \end{aligned} \quad (5)$$

with $\Delta^{\mu\nu} = g^{\mu\nu} - u^\mu u^\nu$ and ϵ, P, u^μ are respectively energy density, pressure density, four velocity of the matter. By applying appropriate projection operators, the candidates of right hand side of the Eq. (5) can be extracted from $T^{\mu\nu}$ as

$$\left\{ \begin{array}{c} \epsilon \\ P \\ K^\rho \\ \pi^{\rho\sigma} \end{array} \right\} = \left\{ \begin{array}{c} u^\mu u^\nu \\ -\frac{1}{3} \Delta^{\mu\nu} \\ \Delta^{\rho\mu} u_\nu \\ (\Delta^{\rho\sigma} \Delta^{\mu\nu} - \frac{1}{3} \Delta^{\rho\mu} \Delta^{\sigma\nu}) \end{array} \right\} T_{\mu\nu}. \quad (6)$$

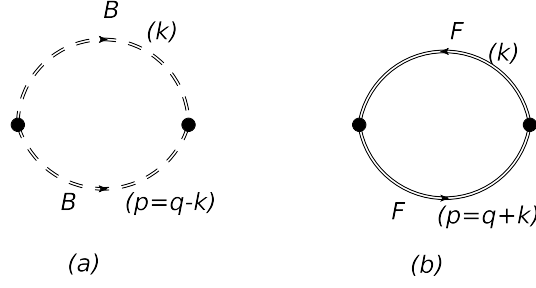


Figure 1: Boson-Boson (a) and Fermion-Fermion (b) loop diagram after Wick contraction from two point function of corresponding viscous-stress tensor.

For ϕ boson and ψ fermion the viscous-stress tensor can be deduced as (see Appendix A)

$$\pi_{\mu\nu} = (\Delta_{\mu}^{\rho}\Delta_{\nu}^{\sigma} - \frac{1}{3}\Delta_{\mu\nu}\Delta^{\rho\sigma}) \left\{ \frac{\partial_{\rho}\phi\partial_{\sigma}\phi}{i\psi\gamma_{\rho}\partial_{\sigma}\psi} \right\}. \quad (7)$$

In RTF, the thermal average of any two point function always give a 2×2 matrix structure. Hence the two point correlator of viscous-stress tensor will be

$$\Pi_{ab}(q) = i \int d^4x e^{iqx} \langle T_c \pi_{\mu\nu}(x) \pi^{\mu\nu}(0) \rangle_{\beta}^{ab}, \quad (8)$$

where the superscripts $a, b (a, b = 1, 2)$ represent the (thermal) indices of the matrix and T_c denotes time ordering with respect to a contour in the complex time plane. Of the variety of possible contours in the complex time plane [19], two are specially interesting, namely the closed one [20] and the symmetrical one [21, 22]. Here the latter contour is chosen.

The matrix can be diagonalized in terms of a single analytic function which determines completely the dynamics of the corresponding two point function. The diagonal element can also be related with the retarded two point function of viscous-stress tensor. These retarded function, $\Pi^R(q)$ (say) or diagonal element, $\bar{\Pi}(q)$ (say) is simply related to any one component, say 11 component of the matrix. The relation among the imaginary part of these components (for $\phi\phi$ or $\psi\psi$ loops) is

$$\text{Im}\Pi^R(q) = \epsilon(q_0)\text{Im}\bar{\Pi}(q) = \tanh(\frac{\beta q_0}{2})\text{Im}\Pi_{11}(q). \quad (9)$$

Now the imaginary part of retarded two point function of any field quantity is directly related with the corresponding spectral function. For our present case, the viscous-stress tensor $\pi_{\mu\nu}$ is the field quantity. Hence the relation between corresponding spectral function $A_{\eta}(q)$ and retarded function $\Pi^R(q)$ is given by

$$A_{\eta}(q) = 2\text{Im}\Pi^R(q). \quad (10)$$

Using this relation, the Eq. (1)) become

$$\eta = \frac{1}{10} \lim_{q_0, \vec{q} \rightarrow 0} \frac{\text{Im}\Pi^R(q_0, \vec{q})}{q_0}. \quad (11)$$

To calculate this retarded two point function, let us start from 11 component of the Π_{ab} matrix. After using Eq. (7) in Eq. (8), the Wick contraction of the boson fields (ϕ) and fermion fields (ψ)

generate an one-loop kind of skeleton diagram, which are shown in Fig. 1(a) and (b) respectively. They can be mathematically expressed as [23]

$$\Pi_{11}(q) = i\epsilon_F \int \frac{d^4k}{(2\pi)^4} N(q, k) D_{11}(k) D_{11}(p), \quad (12)$$

where $D_{11}(k)$ and $D_{11}(p)$ are the scalar part of the propagators at finite temperature. Now $p = q - k$ for boson-boson ($\phi\phi$) loop whereas $p = q + k$ for fermion-fermion ($\psi\psi$) loop. In fermion loop there must be an extra negative sign according to Feynman rule, which is maintained by putting $\epsilon_F = +, -$ for $\phi\phi$ and $\psi\psi$ loops respectively. The term $N(q, k)$ contain the numerator part of two propagators as well as the vertex kind of part which is determined from Eq. (7). The expression of $N(q, k)$ (multiplying with the ϵ_F) for $\phi\phi$ and $\psi\psi$ loop are respectively given by (see Appendix B)

$$\epsilon_F N(q, k) = -[\vec{k}^2(\vec{q} - \vec{k})^2 + \frac{\{\vec{k} \cdot (\vec{q} - \vec{k})\}^2}{3}] \quad (13)$$

and

$$\epsilon_F N(q, k) = -\frac{32}{3} \{k_0(q_0 + k_0)\} \{\vec{k} \cdot (\vec{q} + \vec{k})\} + 4[\{\vec{k} \cdot (\vec{q} + \vec{k})\}^2 + \frac{\vec{k}^2(\vec{q} + \vec{k})^2}{3}]. \quad (14)$$

Just by absorbing the ϵ_F in $N(q, k)$ we will not write it for our further calculations.

In RTF, the 11 component of the scalar part of the thermal propagator can be expressed as

$$\begin{aligned} D^{11}(k) &= \frac{-1}{k_0^2 - \omega_k^2 + i\epsilon} + 2\pi i \epsilon_k F_k(k_0) \delta(k_0^2 - \omega_k^2), \text{ with } F_k(k_0) = n_k^+ \theta(k_0) + n_k^- \theta(-k_0) \\ &= -\frac{1}{2\omega_k} \left(\frac{1 - n_k^+}{k_0 - \omega_k + i\epsilon} + \frac{n_k^+}{k_0 - \omega_k - i\epsilon} - \frac{1 - n_k^-}{k_0 + \omega_k - i\epsilon} - \frac{n_k^-}{k_0 + \omega_k + i\epsilon} \right). \end{aligned} \quad (15)$$

Here $n_k^\pm(\omega_k) = \frac{1}{e^{\beta(\omega_k \mp \mu)} - \epsilon_k}$ ($\epsilon_k = +1, -1$ for ϕ and ψ respectively) is the thermal distribution of ϕ with energy $\omega_k = (\vec{k}^2 + m_\phi^2)^{1/2}$ or ψ with energy $\omega_k = (\vec{k}^2 + m_\psi^2)^{1/2}$, where the \pm sign in the superscript of n_k refer to particle and anti-particle respectively.

After doing the k_0 integration of Eq. (12) and then using the relations (9), we get the imaginary part of retarded self-energy [24]

$$\begin{aligned} \text{Im}\Pi^R(q) &= \int \frac{d^3k}{(2\pi)^3} \frac{(-\pi)N}{4\omega_k\omega_p} [C_1\delta(q_0 - \omega_k - \omega_p) + C_2\delta(q_0 - \omega_k + \omega_p) \\ &\quad + C_3\delta(q_0 + \omega_k - \omega_p) + C_4\delta(q_0 + \omega_k + \omega_p)], \end{aligned} \quad (16)$$

where $\omega_p = \sqrt{(\vec{q} \mp \vec{k})^2 + m^2}$ (\mp for $\phi\phi$ and $\psi\psi$ loop respectively) and $N = N(k_0 = \pm\omega_k, \vec{k}, q)$. Here C_i ($i = 1, \dots, 4$) are four different statistical probability attached with four different delta functions. For $\phi\phi$ loop, C_i ($i = 1, \dots, 4$) = $\{1 + n_k^+(\omega_k) + n_p^+(q_0 - \omega_k)\}$, $\{-n_k^+(\omega_k) + n_p^-(q_0 + \omega_k)\}$, $\{n_k^-(\omega_k) - n_p^+(q_0 + \omega_k)\}$, $\{-1 - n_k^-(\omega_k) - n_p^-(q_0 - \omega_k)\}$ whereas C_i ($i = 1, \dots, 4$) = $\{-1 + n_k^-(\omega_k) + n_p^+(q_0 + \omega_k)\}$, $\{-n_k^-(\omega_k) + n_p^-(q_0 + \omega_k)\}$, $\{n_k^+(\omega_k) - n_p^+(q_0 + \omega_k)\}$, $\{1 - n_k^+(\omega_k) - n_p^-(q_0 - \omega_k)\}$ for $\psi\psi$ loop. Four different branch cuts in the real axis of complex q_0 plane can be identified from four different terms of $\text{Im}\Pi^R(q)$ with different delta functions. In addition to the unitary cut, present already in vacuum, the thermal field theory calculation generates a new cut, the so called the Landau cut. The region of these different branch cuts are $(-\infty$ to $-\sqrt{\vec{q}^2 + 4m_{\phi,\psi}^2})$ for unitary cut in negative q_0 -axis, $(-\vec{q}$ to $\vec{q})$ for Landau cut and $(\sqrt{\vec{q}^2 + 4m_{\phi,\psi}^2}$ to $\infty)$ for unitary cut in positive q_0 -axis. Now to calculate η from the $\Pi^R(q)$, we have to concentrate on the limit of $q_0, \vec{q} \rightarrow 0$. Therefore the

Landau cuts will be only the focus of our calculation. Hence using the Landau part of Eq. (16) in Eq. (11), we have

$$\begin{aligned}
\eta &= \frac{1}{10} \lim_{q_0, \vec{q} \rightarrow 0} \frac{1}{q_0} \int \frac{d^3 k}{(2\pi)^3} \frac{(-\pi)N}{4\omega_k \omega_p} \{C_2 \delta(q_0 - \omega_k + \omega_p) + C_3 \delta(q_0 + \omega_k - \omega_p)\} \\
&= \frac{1}{10} \lim_{q_0, \vec{q} \rightarrow 0} \text{Im} \left[\int \frac{d^3 k}{(2\pi)^3} \frac{N}{4\omega_k \omega_p} \lim_{\Gamma \rightarrow 0} \left\{ \frac{C_2/q_0}{(q_0 - \omega_k + \omega_p) + i\Gamma} + \frac{C_3/q_0}{(q_0 + \omega_k - \omega_p) + i\Gamma} \right\} \right] .
\end{aligned} \tag{17}$$

To get a non-divergent contribution of η , the further calculation will be continued for finite value of Γ . This is the place where the interaction scenario is introduced, which is very essential for a dissipative system. This is done by transforming the delta functions for free theory to the spectral functions with finite thermal width for interacting theory. The Γ is identified as the thermal width (or collision rate) of the constituent particles and it reciprocally measures the dissipative coefficients like the shear viscosity. In this respect this formalism may be equivalent to quasi particle approximation and this trained is widely used for calculating the dissipative coefficients in Kubo approach [3, 6]. Using the limiting values,

$$\lim_{\vec{q} \rightarrow 0} \omega_p = \omega_k \tag{18}$$

in Eq. (17), we have

$$\eta = \frac{1}{10} \int \frac{d^3 k}{(2\pi)^3} \frac{(-N^0)}{4\omega_k^2 \Gamma} [I_2 + I_3] , \tag{19}$$

where

$$N^0 = \lim_{q_0, \vec{q} \rightarrow 0} N(k_0 = \pm\omega_k, \vec{k}, q) \tag{20}$$

and

$$I_{2,3} = \lim_{q_0 \rightarrow 0} \frac{C_{2,3}(q_0)}{q_0} , \tag{21}$$

with

$$C_{2,3}(q_0) = \mp n_k^\pm(\omega_k) \pm n_p^\mp(\mp q_0 + \omega_k) . \tag{22}$$

Here in Eq. (21), we see that the limiting value of $I_{2,3}$ is appeared to be a 0/0 form and so we can apply the L'Hospital's rule i.e.

$$\begin{aligned}
I_{2,3} &= \lim_{q_0 \rightarrow 0} \frac{\frac{d}{dq_0} \{C_{2,3}(q_0)\}}{\frac{d}{dq_0} \{q_0\}} \\
&= \beta n_k^\mp (1 + \epsilon_k n_k^\pm) ,
\end{aligned} \tag{23}$$

since

$$\begin{aligned}
\frac{d}{dq_0} \{\pm n_p^\mp(\omega_q = \mp q_0 + \omega_k)\} &= \pm \frac{-\beta \frac{d\omega_q}{dq_0} e^{\beta(\omega_q \pm \mu)}}{\{e^{\beta(\omega_q \pm \mu)} - \epsilon_k\}^2} \\
\lim_{q_0 \rightarrow 0} \frac{d}{dq_0} \{\pm n_p^\mp(\omega_q = \mp q_0 + \omega_k)\} &= \pm \frac{-\beta(\mp) e^{\beta(\omega_k \pm \mu)}}{\{e^{\beta(\omega_k \pm \mu)} - \epsilon_k\}^2} \\
&= \beta [n_k^\pm (1 + \epsilon_k n_k^\pm)] .
\end{aligned} \tag{24}$$

Depending on the sign of ϵ_k , the statistical probability become Bose enhanced ($\epsilon_k = +1$ for ϕ) or Pauli blocked ($\epsilon_k = -1$ for ψ) probability. Hence using Eq. (23) in Eq. (19), we can get a generalized expression of shear viscosity coefficient for ϕ boson or ψ fermion,

$$\begin{aligned}\eta &= \frac{\beta}{10} \int \frac{d^3k}{(2\pi)^3} \frac{(-N^0)}{4\omega_k^2\Gamma} [n_k^-(1 + \epsilon_k n_k^-) + n_k^+(1 + \epsilon_k n_k^+)] \\ &= \frac{\beta}{80\pi^2} \int \frac{\vec{k}^2 d\vec{k}}{\omega_k^2} \frac{(-N^0)}{\Gamma} [n_k^-(1 + \epsilon_k n_k^-) + n_k^+(1 + \epsilon_k n_k^+)] .\end{aligned}\quad (25)$$

From the final expression we can understand the importance of finite value of Γ to get a non-divergent value of η . A finite small value of Γ can be introduced through Dyson's series expansion of a propagator and we can repeat our calculation from Eq. (15) by using $i\Gamma$ in place of $i\eta$. The corresponding Γ for ϕ and ψ can be quantitatively defined as

$$\Gamma_\phi = -\text{Im}\Pi_{(\phi)}^R(k_0 = \omega_k, \vec{k})/m_\phi \quad (\text{for } \phi) , \quad (26)$$

$$\Gamma_\psi = -\text{Im}\Sigma_{(\psi)}^R(k_0 = \omega_k, \vec{k}) \quad (\text{for } \psi) , \quad (27)$$

where $\text{Im}\Pi_{(\phi)}^R(k)$ and $\text{Im}\Sigma_{(\psi)}^R(k)$ are the imaginary part of retarded self-energy for ϕ and ψ respectively, which will be even functions of k_0 .

Let us now concentrate on the Eq. (20) to deduce N^0 . In this limiting case ($q_0, \vec{q} \rightarrow 0$), the Eq. (13) and (14) can be simplified as

$$N^0 = -\frac{4\vec{k}^4}{3} \quad \text{for } \phi\phi \text{ loop} \quad (28)$$

and

$$N^0 = -\frac{16\vec{k}^4}{3} \quad \text{for } \psi\psi \text{ loop} . \quad (29)$$

Hence the shear viscosity of the medium with bosons (ϕ) and fermions (ψ) are respectively given below

$$\begin{aligned}\eta_\phi &= \frac{\beta}{30\pi^2} \int_0^\infty \frac{d\vec{k}\vec{k}^6}{\omega_k^2\Gamma_\phi} \frac{\{n_k^+(1 + n_k^+) + n_k^-(1 + n_k^-)\}}{2} \quad \text{for } \phi\phi \text{ loop} \\ &= \frac{\beta}{30\pi^2} \int_0^\infty \frac{d\vec{k}\vec{k}^6}{\omega_k^2\Gamma_\phi} n_k(1 + n_k) \quad (\text{at } \mu = 0)\end{aligned}\quad (30)$$

and

$$\eta_\psi = \frac{\beta}{15\pi^2} \int_0^\infty \frac{d\vec{k}\vec{k}^6}{\omega_k^2\Gamma_\psi} \{n_k^+(1 - n_k^+) + n_k^-(1 - n_k^-)\} \quad \text{for } \psi\psi \text{ loop} . \quad (31)$$

Some special cases : Now taking isospin degeneracy factor $I_\pi = 3$ for pionic medium we can generate the expression of [3, 6, 22, 23],

$$\eta_\pi = \frac{\beta}{10\pi^2} \int_0^\infty \frac{d\vec{k}\vec{k}^6}{\omega_k^2\Gamma_\pi} n_k(1 + n_k) , \quad (32)$$

where $n_k = n_k^\pm$ for $\mu_\pi = 0$ has to be considered. This one-loop expression of shear viscosity from Kubo approach [3, 6, 23] is exactly coincide with the expressions from the relaxation-time approximation of the kinetic theory approach [25, 26, 27, 23].

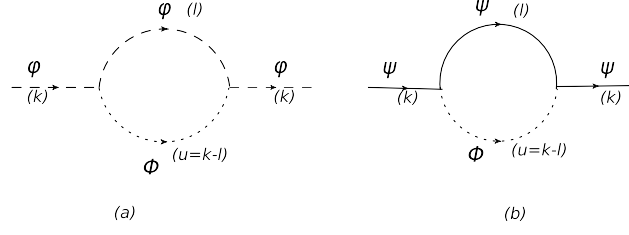


Figure 2: Self-energy of ϕ boson for $\phi\Phi$ loop (a) and self-energy of ψ fermion for $\psi\Phi$ loop (b).

When the constituent particles are nucleon, then we have to take isospin degeneracy $I_N = 2$ in Eq. (31) i.e.

$$\eta_N = \frac{2\beta}{15\pi^2} \int_0^\infty \frac{d\vec{k} \vec{k}^6}{\omega_k^2 \Gamma_N} \{n_k^+(1 - n_k^+) + n_k^-(1 - n_k^-)\} . \quad (33)$$

Similarly for 2-flavor ($N_f = 2$) quark matter the degeneracy factor become $N_f N_c = 6$ (as color degeneracy $N_c = 3$) and so

$$\eta_Q = \frac{2\beta}{5\pi^2} \int_0^\infty \frac{d\vec{k} \vec{k}^6}{\omega_k^2 \Gamma_Q} \{n_k^+(1 - n_k^+) + n_k^-(1 - n_k^-)\} . \quad (34)$$

This expression is also exactly coincide with the expressions from the relaxation-time approximation [28].

3 Calculation of Γ

Let us take a simple ϕ^3 -type interaction Lagrangian density,

$$\mathcal{L} = -g\phi\phi\Phi , \quad (35)$$

by which we can get an estimation of Γ_ϕ for boson constituent particle, ϕ . The Φ is another higher mass boson like ϕ . The self-energy of ϕ for $\phi\Phi$ loop (as shown in Fig. 2(a)) can be derived in RTF with the help of the above Lagrangian. Owing to the cutkosky rule at finite T , the Γ_ϕ can be extracted from the imaginary part of this one-loop self-energy of ϕ at its pole, which is already expressed in Eq. (26).

For estimating Γ_ϕ , we have to repeat a similar calculations as previously done in one-loop calculation for η . Therefore Let us start from 11 component of self-energy of ϕ for $\phi\Phi$ loop,

$$\Pi_{(\phi)}^{11}(k) = -i \int \frac{d^4 l}{(2\pi)^4} L(k, l) D_{11}(l, m_\phi) D_{11}(u = k - l, m_\Phi) , \quad (36)$$

where $D_{11}(l, m_\phi)$ and $D_{11}(u = k - l, m_\Phi)$ are the scalar part of ϕ and Φ propagators at finite temperature with similar form like Eq. (15).

Similar to Eq. (16), we will get the imaginary part of retarded self-energy for the $\phi\Phi$ loop,

$$\begin{aligned} \text{Im}\Pi_{(\phi)}^R(k) &= \pi \int \frac{d^3 l}{(2\pi)^3} \frac{1}{4\omega_l \omega_u} [L(l_0 = \omega_l, \vec{l}, k) [\{1 + n_l(\omega_l) + n_u(k_0 - \omega_l)\} \delta(k_0 - \omega_l - \omega_u) \\ &\quad + \{-n_l(\omega_l) + n_u(-k_0 + \omega_l)\} \delta(k_0 - \omega_l + \omega_u)] \\ &\quad + L(l_0 = -\omega_l, \vec{l}, k) [\{n_l(\omega_l) - n_u(k_0 + \omega_l)\} \delta(k_0 + \omega_l - \omega_u) \\ &\quad + \{-1 - n_l(\omega_l) - n_u(-k_0 - \omega_l)\} \delta(k_0 + \omega_l + \omega_u)] , \end{aligned} \quad (37)$$

where $\omega_u = \sqrt{(\vec{k} - \vec{l})^2 + m_\Phi^2}$ and n 's are Bose-Einstein distribution functions. The region of the different branch cuts in k_0 -axis are $(-\infty \text{ to } -\sqrt{\vec{k}^2 + (m_\Phi + m_\phi)^2})$ for unitary cut in negative k_0 -axis, $(-\sqrt{\vec{k}^2 + (m_\Phi - m_\phi)^2} \text{ to } \sqrt{\vec{k}^2 + (m_\Phi - m_\phi)^2})$ for Landau cut and $(\sqrt{\vec{k}^2 + (m_\Phi + m_\phi)^2} \text{ to } \infty)$ for unitary cut in positive k_0 -axis. These are the different off-shell regions of ϕ boson, where imaginary part of its self-energy acquires a non-zero values because of the different δ functions in Eq. (37). One can notice that the ϕ pole will remain within the Landau cuts only when $m_\Phi > 2m_\phi$. Hence we take an ad hoc assumption $m_\Phi = 3m_\phi$ to satisfy the threshold condition.

According to Eq. (26), the Γ_ϕ will be coming from Landau cut contribution associated with the third term of Eq. (37), which can be simplified as

$$\Gamma_\phi = \frac{1}{16\pi\vec{k}m_\phi} \int_{\tilde{\omega}^+}^{\tilde{\omega}^-} d\tilde{\omega} L(l_0 = -\tilde{\omega}, \vec{l} = \sqrt{\tilde{\omega}^2 - m_\phi^2}, k_0 = \omega_k, \vec{k}) \{n_l(\tilde{\omega}) - n_u(\omega_k + \tilde{\omega})\}, \quad (38)$$

where $\tilde{\omega}^\pm = \frac{R^2}{2m_\phi^2}(-\omega_k \pm \vec{k}W)$ with $\omega_k = \sqrt{\vec{k}^2 + m_\phi^2}$, $W = \sqrt{1 - \frac{4m_\phi^4}{R^4}}$ and $R^2 = 2m_\phi^2 - m_\Phi^2$.

Now to estimate Γ_ψ of ψ fermion, let us take a similar kind of interaction Lagrangian density,

$$\mathcal{L} = -G\bar{\psi}\psi\Phi, \quad (39)$$

where the mass of the Φ boson is again assumed to be three times larger than the mass of the ψ fermion i.e. $m_\Phi = 3m_\psi$. The self-energy of ψ , $\Sigma_{(\psi)}(k)$ for $\psi\Phi$ loop is shown in Fig. 2(b). According to Eq. (27), we get

$$\Gamma_\psi = \frac{1}{16\pi\vec{k}} \int_{\tilde{\omega}^+}^{\tilde{\omega}^-} d\tilde{\omega} L(l_0 = -\tilde{\omega}, \vec{l} = \sqrt{\tilde{\omega}^2 - m_\psi^2}, k_0 = \omega_k, \vec{k}) \{n_l^-(\tilde{\omega}) + n_u(\omega_k + \tilde{\omega})\}, \quad (40)$$

which is very similar to Eq. (38). The modified parameters are $\tilde{\omega}^\pm = \frac{R^2}{2m_\psi^2}(-\omega_k \pm \vec{k}W)$ with $\omega_k = \sqrt{\vec{k}^2 + m_\psi^2}$, $W = \sqrt{1 - \frac{4m_\psi^4}{R^4}}$ and $R^2 = 2m_\psi^2 - m_\Phi^2$. Here n_l^- is Fermi-Dirac distribution function of anti-fermion and n_u is Bose-Einstein distribution function of Φ boson.

The vertex part $L(k, l)$ for these loops are respectively given below

$$L(k, l) = -g^2 \quad (\text{for } \phi\Phi \text{ loop}), \quad (41)$$

$$L(k, l) = -G^2 m_\psi \quad (\text{for } \psi\Phi \text{ loop}). \quad (42)$$

4 Higher order loop diagrams

As $\Gamma_\phi \propto g^2$ (or $\Gamma_\psi \propto G^2$), hence our one-loop contribution of two point viscous stress tensor will be $\mathcal{O}(1/g^2)$ (since $\eta \propto \mathcal{O}(1/\Gamma_\phi)$). Now there are some higher order loop diagrams which are also $\mathcal{O}(1/g^2)$. First possible digram is shown in the Fig. 3(a) which contain two loops and two $\phi\phi\Phi$ vertex $v_{\phi\phi\Phi} \propto g$. Therefore its order will be $\mathcal{O}(\frac{1}{\Gamma^2} v_{\phi\phi\Phi}^2) = \mathcal{O}(1/g^2)$ (as $1/\Gamma$ will be coming from each loop). Similarly we can get same order from the diagram, shown in the Fig. 3(b), which contain $(n+1)$ number of loops and $2n$ number of $v_{\phi\phi\Phi}$. Even for $n = \infty$ we get same order of contribution. Let us first derive the two-loop digram (Fig. 3(a)) to get a numerical estimation, which can be compared with the contributions of one-loop diagram. Instead of 11 component we will deduce the 12 component for some certain advantage to simplify our calculation. As any one

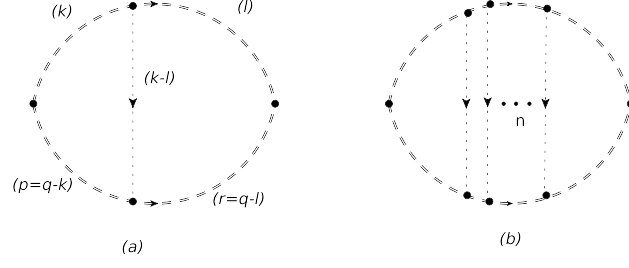


Figure 3: two loops (a) and $(n+1)$ loops (b) ladder type diagrams for $\phi\phi\Phi$ interaction.

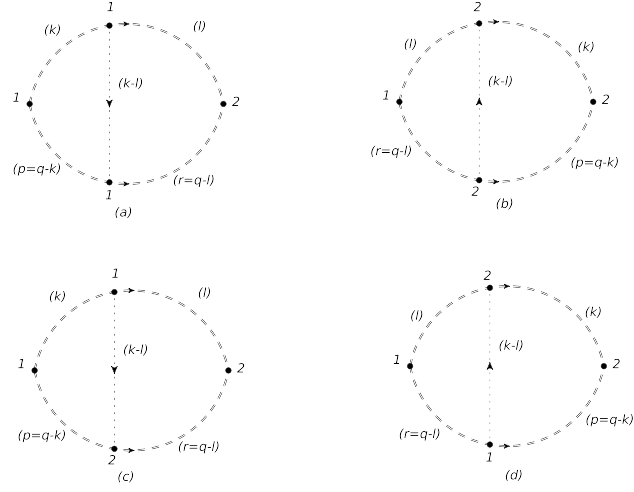


Figure 4: The four possible combinations for two loop diagrams in RTF. The Π_{12}^{AB} is the combinations of diagrams (a) and (b) whereas diagrams (c) and (d) are combined in Π_{12}^{CD} .

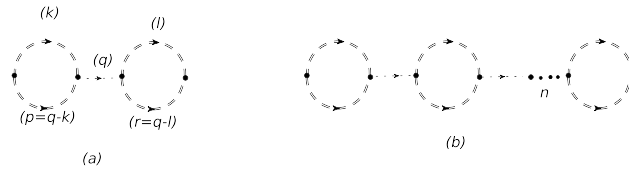


Figure 5: two loops (a) and $(n+1)$ loops (b) rung type diagrams for $\phi\phi\Phi$ interaction.

of the four component in RTF can be expressed in terms of the diagonal element $\bar{\Pi}$ due to their relation

$$\begin{pmatrix} \Pi_{11} & \Pi_{12} \\ \Pi_{21} & \Pi_{22} \end{pmatrix} = \begin{pmatrix} \sqrt{1+n} & -\sqrt{n} \\ -\sqrt{n} & \sqrt{1+n} \end{pmatrix} \begin{pmatrix} \bar{\Pi} & 0 \\ 0 & -\bar{\Pi}^* \end{pmatrix} \begin{pmatrix} \sqrt{1+n} & -\sqrt{n} \\ -\sqrt{n} & \sqrt{1+n} \end{pmatrix}. \quad (43)$$

Therefore we can express the shear viscosity in terms of 12 component of two-loop skeleton digram as

$$\eta^{(2)} = \frac{1}{10} \lim_{q_0, \vec{q} \rightarrow 0} \frac{\epsilon(q_0) \text{Im} \bar{\Pi}^{(2)}(q_0, \vec{q})}{q_0} = \frac{1}{10} \lim_{q_0, \vec{q} \rightarrow 0} \frac{\sinh(\beta q_0/2)}{q_0} \text{Im} \Pi_{12}^{(2)}(q_0, \vec{q}). \quad (44)$$

Applying L'Hospital's rule, we have

$$\begin{aligned} \lim_{q_0 \rightarrow 0} \frac{\sinh(\beta q_0/2)}{q_0} &= \lim_{q_0 \rightarrow 0} \frac{\frac{d}{dq_0} \{\sinh(\beta q_0/2)\}}{\frac{d}{dq_0} \{q_0\}} \\ &= \frac{\beta}{2} \end{aligned} \quad (45)$$

and so

$$\eta^{(2)} = \frac{\beta}{20} \lim_{q_0, \vec{q} \rightarrow 0} \text{Im} \Pi_{12}^{(2)}(q_0, \vec{q}). \quad (46)$$

Denoting the intermediate vertices $v_{\phi\phi\Phi}$ in four possible way as shown in Fig. (4), we get the 12 component as a summation of four possible diagrams. By attaching different momentum labels on the internal lines, the four terms can be merged into two as given below [29]

$$i\Pi_{12}^{(2)}(q) = i\Pi_{12}^{AB}(q) + i\Pi_{12}^{CD}(q), \quad (47)$$

where

$$i\Pi_{12}^{AB}(q) = -i \int \frac{d^4 k d^4 l}{(2\pi)^8} N^{(2)}(q, k, l) D_{12}^\phi(l) D_{21}^\phi(r = q - l) D^{AB}, \quad (48)$$

$$i\Pi_{12}^{CD}(q) = i \int \frac{d^4 k d^4 l}{(2\pi)^8} N^{(2)}(q, k, l) D_{12}^\phi(l) D_{21}^\phi(p = q - k) D_{12}^\Phi(u = k - l) D^{CD}, \quad (49)$$

with

$$\begin{aligned} D^{AB} &= \{D_{11}^\phi(k) D_{11}^\phi(p = q - k) D_{11}^\Phi(u = k - l) + D_{22}^\phi(k) D_{22}^\phi(p = q - k) D_{22}^\Phi(u = k - l)\} \\ &= 2i \text{Im} \{D_{11}^\phi(k) D_{11}^\phi(p = q - k) D_{11}^\Phi(u = k - l)\}, \end{aligned} \quad (50)$$

$$\begin{aligned} D^{CD} &= \{D_{11}^\phi(k) D_{22}^\phi(r = q - l) + D_{22}^\phi(k) D_{11}^\phi(r = q - l)\} \\ &= 2\text{Re} \{D_{11}^\phi(k) D_{22}^\phi(r = q - l)\}. \end{aligned} \quad (51)$$

The above simplifications have been done by using the identity $D_{11} = -D_{22}^*$. The $N^{(2)}$ in the limit of $q_0, \vec{q} \rightarrow 0$ can be expressed as

$$N^{(2)} = -\frac{4}{3} g^2 \vec{k}^2 \vec{l}^2, \quad (52)$$

where the angle between \vec{k} and \vec{l} is fixed to zero for simplifying the calculations because our main purpose in this section is just to estimate the order of magnitude for the two-loop contribution in shear viscosity.

Now using the 12 component of scalar propagator,

$$D_{12}^l = D_{21}^l = 2\pi i F_l \delta(l_0^2 - \omega_l^2), \quad F_l = \sqrt{n_l(1 + n_l)} \quad (53)$$

in Eq. (48), we have

$$\Pi_{12}^{AB}(q) = \frac{-4i}{3} \int \frac{d^4 l}{(2\pi)^4} (\vec{l}^2) [2\pi F_l \delta(l_0^2 - \omega_l^2)] [2\pi F_r \delta((q_0 - l_0)^2 - \omega_r^2)] \{I^{AB}\} , \quad (54)$$

where

$$I^{AB} = 2\text{Im}G, \quad G = \int \frac{d^4 k (\vec{k}^2 g^2)}{(2\pi)^4} \{D_{11}^\phi(k) D_{11}^\phi(p = q - k) D_{11}^\Phi(u = k - l)\} . \quad (55)$$

After performing the l_0 integration, the Landau cut contribution¹ of $\Pi_{12}^{AB}(q)$ is given by

$$\begin{aligned} \Pi_{12}^{AB}(q) &= \frac{-4}{3} i \int \frac{d^3 l}{(2\pi)^3} \frac{\pi \vec{l}^2 F_l F_r}{2\omega_l \omega_r} [I^{AB}(l_0 = \omega_l) \delta(q_0 - \omega_l + \omega_r) + I^{AB}(l_0 = -\omega_l) \delta(q_0 + \omega_l - \omega_r)] \\ &= \frac{-4}{3} i \int \frac{d^3 l}{(2\pi)^3} \frac{\vec{l}^2 F_l F_r}{2\omega_l \omega_r} \lim_{\Gamma_\phi \rightarrow 0} \left[\frac{\Gamma_\phi}{(q_0 - \omega_l + \omega_r)^2 + \Gamma_\phi^2} \{I^{AB}(l_0 = \omega_l)\} \right. \\ &\quad \left. + \frac{\Gamma_\phi}{(q_0 + \omega_l - \omega_r)^2 + \Gamma_\phi^2} \{I^{AB}(l_0 = -\omega_l)\} \right] . \end{aligned} \quad (56)$$

Again starting with free theory ($\Gamma_\phi \rightarrow 0$), we will make our calculations convert to interacting theory just by keeping Γ_ϕ as a non-zero value. In the limit of $q_0, \vec{q} \rightarrow 0$, $\omega_r \rightarrow \omega_l$ and $n_r \rightarrow n_l$. So

$$\lim_{q_0, \vec{q} \rightarrow 0} \Pi_{12}^{AB}(q) = \frac{-4i}{3} \int \frac{d^3 l}{(2\pi)^3} \frac{\vec{l}^2 F_l^2}{2\omega_l^2 \Gamma_\phi} \lim_{q_0, \vec{q} \rightarrow 0} \{I^{AB}(l_0 = \omega_l) + I^{AB}(l_0 = -\omega_l)\} . \quad (57)$$

Now we concentrate on $I^{AB} = 2\text{Im}G$, where G can be evaluated as

$$\begin{aligned} G &= - \int \frac{d^3 k}{(2\pi)^3} \frac{\vec{k}^2 g^2}{4\omega_k \omega_p} \{n_k(1 + n_p) + n_p(1 + n_k)\} \left[\frac{\Gamma_\phi}{(q_0 - \omega_k + \omega_p)^2 + \Gamma_\phi^2} D_{11}^\Phi(u_0 = \omega_k - l_0) \right. \\ &\quad \left. + \frac{\Gamma_\phi}{(q_0 + \omega_k - \omega_p)^2 + \Gamma_\phi^2} D_{11}^\Phi(u_0 = -\omega_k - l_0) \right] . \end{aligned} \quad (58)$$

Here also we have taken the Landau cut contribution for finite Γ_ϕ after performing the k_0 integration. One can find that the calculation of G is very similar to the calculation of 11 component of self-energy for finite Γ_ϕ if we approximately assume $\vec{k}^2 D_{11}^\Phi$ as a vertex part. In the limiting case,

$$\lim_{q_0, \vec{q} \rightarrow 0} G = - \int \frac{d^3 k}{(2\pi)^3} \frac{\vec{k}^2 g^2 n_k(1 + n_k)}{2\omega_k^2 \Gamma_\phi} [D_{11}^\Phi(u_0 = \omega_k - l_0) + D_{11}^\Phi(u_0 = -\omega_k - l_0)] . \quad (59)$$

As

$$\text{Im}D_{11}^\Phi(u) = \frac{\pi n_u(\omega_u)}{\omega_u} \{\delta(u_0 - \omega_u) + \delta(u_0 + \omega_u)\} , \quad (60)$$

therefore

$$\begin{aligned} \lim_{q_0, \vec{q} \rightarrow 0} I^{AB}(l_0) &= -2 \int \frac{d^3 k}{(2\pi)^3} \frac{\vec{k}^2 g^2 n_k(1 + n_k)}{2\omega_k^2 \Gamma_\phi} \frac{\pi n_u}{\omega_u} \{\delta(l_0 - \omega_k - \omega_u) \\ &\quad + \delta(l_0 - \omega_k + \omega_u) + \delta(l_0 + \omega_k - \omega_u) + \delta(l_0 + \omega_k + \omega_u)\} . \end{aligned} \quad (61)$$

Here four delta functions provide four different regions in l_0 -axis to $I^{AB}(l_0)$, where the function will remain non-zero. These regions are exactly similar to the non-zero regions of imaginary part

¹As our main focus on $q_0, \vec{q} \rightarrow 0$ for shear viscosity calculations, so we have again considered only Landau cuts and excluded the unitary cut contributions.

of any one-loop self-energy function (see Eq. (37)). For $l_0 = \pm\omega_l$, third and second delta functions respectively contribute with same magnitude. Hence

$$\begin{aligned}\lim_{q_0, \vec{q} \rightarrow 0} I^{AB}(l_0 = \omega_l) &= \lim_{q_0, \vec{q} \rightarrow 0} I^{AB}(l_0 = -\omega_l) \\ &= \frac{-g^2}{4\pi\vec{l}} \int_{\tilde{\omega}^+}^{\tilde{\omega}^-} d\tilde{\omega} \frac{(\tilde{\omega}^2 - m_\pi^2) n_k(\tilde{\omega}) \{1 + n_k(\tilde{\omega})\} n_u(\omega_l + \tilde{\omega})}{\tilde{\omega} \Gamma_\phi},\end{aligned}\quad (62)$$

where $\tilde{\omega}^\pm = \frac{R^2}{2m_\phi^2}(-\omega_l \pm \vec{l}W)$ with $W = \sqrt{1 - \frac{4m_\phi^4}{R^4}}$ and $R^2 = 2m_\phi^2 - m_\Phi^2$. Using (62) in (57) and taking the imaginary part, we have

$$\lim_{q_0, \vec{q} \rightarrow 0} \text{Im}\Pi_{12}^{AB}(q) = \frac{4}{3} \int \frac{d^3l}{(2\pi)^3} \frac{\vec{l}^4 n_l(1 + n_l)}{2\omega_l^2 \Gamma_\phi} 2F^{AB}(\vec{l}, T) \quad (63)$$

where

$$\begin{aligned}F^{AB}(\vec{l}, T) &= \frac{-1}{\vec{l}^2} \lim_{q_0, \vec{q} \rightarrow 0} I^{AB}(l_0 = \omega_l, \vec{l}, T) \\ &= \frac{g^2}{4\pi\vec{l}^3} \int_{\tilde{\omega}^+}^{\tilde{\omega}^-} d\tilde{\omega} \frac{(\tilde{\omega}^2 - m_\pi^2) n_k(\tilde{\omega}) \{1 + n_k(\tilde{\omega})\} n_u(\omega_l + \tilde{\omega})}{\tilde{\omega} \Gamma_\phi}.\end{aligned}\quad (64)$$

Next to calculate Π^{CD} , we will first find

$$\begin{aligned}D^{CD} &= 2\text{Re}\{D_{11}^\pi(k)D_{22}^\pi(r = q - l)\} \\ &= 2 \left[\frac{-1}{k_0^2 - \omega_k^2 + i\epsilon} \frac{1}{(q_0 - l_0)^2 - \omega_r^2 + i\epsilon} \right. \\ &\quad \left. + \{2i\pi n_k \delta(k_0^2 - \omega_k^2)\} \{2i\pi n_r \delta((q_0 - l_0)^2 - \omega_r^2)\} \right],\end{aligned}\quad (65)$$

in which 2nd part can be approximately ignored due to containing exponentially suppressing term $n_k n_r$. Using its first part in Eq. (49), we have

$$\Pi_{12}^{CD}(q) = 2 \int \frac{d^4k}{(2\pi)^4} \frac{(-4\vec{k}^2)}{3} \left[\frac{-1}{k_0^2 - \omega_k^2 + i\epsilon} 2i\pi F_p \delta((q_0 - k_0)^2 - \omega_p^2) \right] I^{CD}, \quad (66)$$

where

$$I^{CD} = \int \frac{d^4l}{(2\pi)^4} (g^2 \vec{l}^2) \left[\frac{D_{12}^\sigma(k - l)}{(q_0 - l_0)^2 - \omega_r^2 + i\epsilon} 2i\pi F_l \delta(l_0^2 - \omega_l^2) \right]. \quad (67)$$

After doing k_0 integration of Eq. (66) and taking the Landau cut contribution with finite Γ_ϕ (in place of ϵ in (66)) we will get

$$\lim_{q_0, \vec{q} \rightarrow 0} \Pi_{12}^{CD}(q) = \frac{4}{3} \int \frac{d^3k}{(2\pi)^3} \frac{\vec{k}^2 F_k}{2\omega_k^2 \Gamma_\phi} \lim_{q_0, \vec{q} \rightarrow 0} \{I^{CD}(k_0 = \omega_k) + I^{CD}(k_0 = -\omega_k)\}, \quad (68)$$

which is very similar to Eq. (57). Going through the similar process for Eq. (67), we have

$$\lim_{q_0, \vec{q} \rightarrow 0} I^{CD}(k_0) = \int \frac{d^3l}{(2\pi)^3} \frac{g^2 \vec{l}^2 F_l}{2\omega_l^2 \Gamma_\phi} \{D_{12}^\Phi(u_0 = k_0 - \omega_l) + D_{12}^\Phi(u_0 = k_0 + \omega_l)\}, \quad (69)$$

which can be compared with (59). Now the imaginary part of Eq. (68) is

$$\lim_{q_0, \vec{q} \rightarrow 0} \text{Im}\Pi_{12}^{CD}(q) = \frac{4}{3} \int \frac{d^3k}{(2\pi)^3} \frac{\vec{k}^2 F_k}{2\omega_k^2 \Gamma_\phi} \lim_{q_0, \vec{q} \rightarrow 0} \{\text{Im}I^{CD}(k_0 = \omega_k) + \text{Im}I^{CD}(k_0 = -\omega_k)\}, \quad (70)$$

where

$$\begin{aligned}\text{Im}I^{CD}(k_0 = \omega_k, \vec{k}) &= \text{Im}I^{CD}(k_0 = -\omega_k, \vec{k}) \\ &= \frac{g^2}{16\pi\vec{k}} \int_{\tilde{\omega}^+}^{\tilde{\omega}^-} d\tilde{\omega} \frac{(\tilde{\omega}^2 - m_\phi^2)F_l(\tilde{\omega})F_u(\omega_k + \tilde{\omega})}{\tilde{\omega}\Gamma_\phi} .\end{aligned}\quad (71)$$

One can notice that the Eq. (71) is very analogous to (62). Using (71) in (70), we have

$$\lim_{q_0, \vec{q} \rightarrow 0} \text{Im}\Pi_{12}^{CD}(q) = \frac{4}{3} \int \frac{d^3k}{(2\pi)^3} \frac{\vec{k}^4 n_k (1 + n_k)}{2\omega_k^2 \Gamma_\phi} 2F^{CD}(\vec{k}, T) , \quad (72)$$

where

$$\begin{aligned}F^{CD}(\vec{k}, T) &= \frac{1}{F_k \vec{k}^2} \lim_{q_0, \vec{q} \rightarrow 0} I^{CD}(k_0 = \omega_k, \vec{k}, T) \\ &= \frac{g^2}{16\pi F_k \vec{k}^3} \int_{\tilde{\omega}^+}^{\tilde{\omega}^-} d\tilde{\omega} \frac{(\tilde{\omega}^2 - m_\pi^2)F_l(\tilde{\omega})F_u(\omega_k + \tilde{\omega})}{\tilde{\omega}\Gamma_\phi} .\end{aligned}\quad (73)$$

Using (63) and (72) in (46) we get the final expression of shear viscosity for two loop diagram as

$$\eta^{(2)} = \frac{\beta}{30\pi^2} \int \frac{d\vec{k} F(\vec{k}, T) \vec{k}^6}{\Gamma_\phi \omega_k^2} n_k (1 + n_k) , \quad (74)$$

where

$$F(\vec{k}, T) = F^{AB}(\vec{k}, T) + F^{CD}(\vec{k}, T) \quad (75)$$

is the main factor which makes the $\eta^{(2)}$ be different from the $\eta^{(1)}$ (let us denote η of Eq. (30) by $\eta^{(1)}$ to mark as one-loop contribution) since Eq. (74) become identical with Eq. (30) for $F(\vec{k}, T) = 1$.

Another pattern of two loop diagram and its nth extension are shown in Fig. 5(a) and (b) respectively. Though these are seems to be contributed with $\mathcal{O}(1/\Gamma_\phi)$ but actually they can be analytically obtained as zero. The two loop diagram in the static limit can be expressed as

$$\begin{aligned}\lim_{q_0, \vec{q} \rightarrow 0} \Pi_{11}^{(2)} &= - \lim_{q_0, \vec{q} \rightarrow 0} \left[\int \frac{d^4k}{(2\pi)^4} N(q, k) D_{11}^\phi(k) D_{11}^\phi(p = q - k) \right] D_{11}^\Phi(q) \\ &\quad \left[\int \frac{d^4l}{(2\pi)^4} N(q, l) D_{11}^\phi(l) D_{11}^\phi(p = q - l) \right] \\ &= - \left[i \int \frac{d^3k}{(2\pi)^3} \frac{-N(\vec{k}) n_k (1 + n_k)}{\Gamma_\phi \omega_k^2} \right] \left[\lim_{q_0, \vec{q} \rightarrow 0} \{\text{Re} D_{11}^\Phi + i \text{Im} D_{11}^\Phi\} \right] \\ &\quad \left[i \int \frac{d^3l}{(2\pi)^3} \frac{-N(\vec{l}) n_l (1 + n_l)}{\Gamma_\phi \omega_l^2} \right] .\end{aligned}\quad (76)$$

Its imaginary part is directly proportional to

$$\lim_{q_0, \vec{q} \rightarrow 0} \text{Im} D_{11}^\Phi = \lim_{q_0, \vec{q} \rightarrow 0} 2\pi n_q^\Phi \delta(q^2 - m_\Phi^2) , \quad (77)$$

which is exactly equal to zero. Therefore $\eta^{(2)}$, which is related with imaginary part of $\Pi_{11}^{(2)}$, is also become zero.

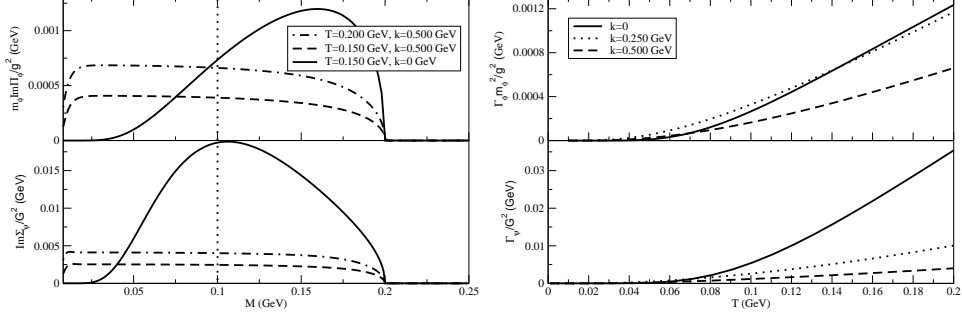


Figure 6: Left : Imaginary part of self-energy of ϕ boson (upper panel) and ψ fermion (lower panel) for different values of three-momentum \vec{k} and temperature T . The dotted line is indicating the pole positions of ϕ boson or ψ fermion ($m_\phi = m_\psi = 0.100$ GeV). Right : the T dependence of thermal widths (Γ_ϕ and Γ_ψ) for ϕ (upper panel) and ψ (lower panel).

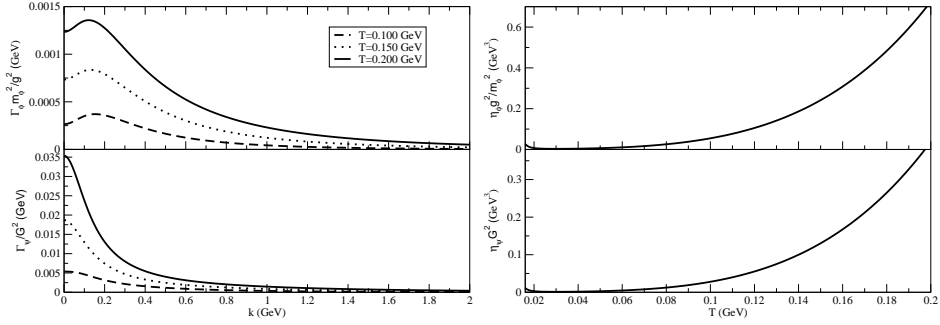


Figure 7: Left : Γ_ϕ (upper panel) and Γ_ψ (lower panel) vs \vec{k} . Right : T dependence of shear viscosity coefficients η_ϕ and η_ψ for ϕ boson (upper panel) and ψ fermion (lower panel) respectively.

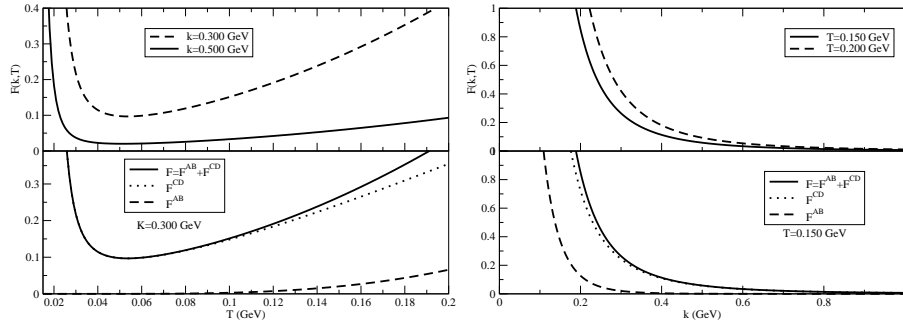


Figure 8: Upper panel : T (left) and \vec{k} (right) dependency of $F(\vec{k}, T)$. Lower panel : T (left) and \vec{k} (right) dependency of individual contributions of F^{AB} (dashed line), F^{CD} (dotted line) and their total F (solid line).

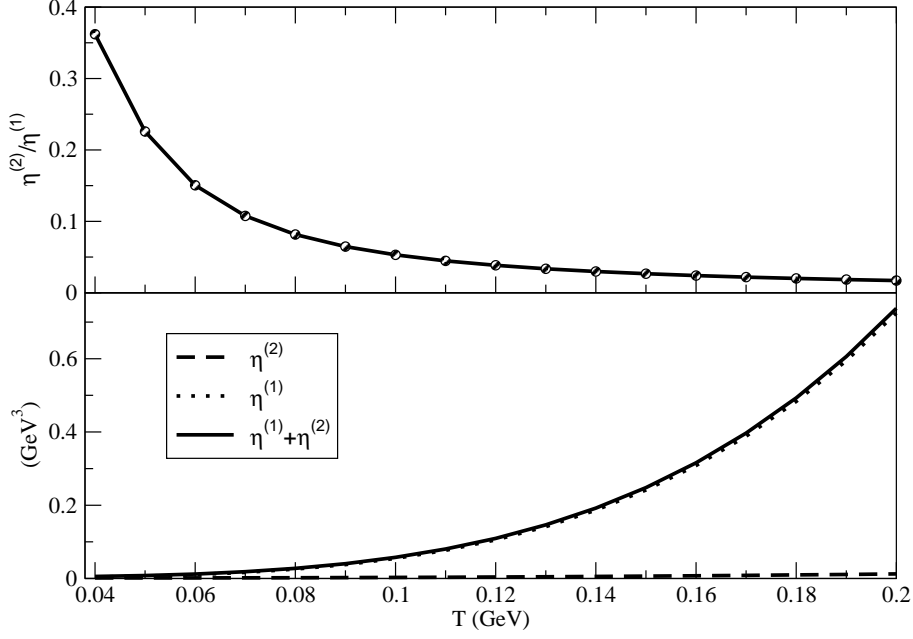


Figure 9: Upper panel : The variation of ratio of two-loop ($\eta^{(2)}$) to one-loop ($\eta^{(1)}$) contributions in shear viscosity with temperature T . Lower panel : T dependency of the individual contribution of $\eta^{(2)}$ (dashed line), $\eta^{(1)}$ (dotted line) and their total (solid line).

5 Numerical discussion

Let us first concentrate on the numerical results of thermal width and then on the results of shear viscosity coefficient. In Sec.(3), we have noticed that thermal width of ϕ boson and ψ fermion are coming from the Landau cut contributions of their corresponding one-loop self-energies which are shown in the left panel of Fig. (6). Here the imaginary part of the ϕ (upper panel) and ψ (lower panel) self-energies are exhibiting their non-zero contributions within the Landau cut regions (from 0 to $(m_\phi - m_{\phi,\psi})$ i.e. from 0 to 0.2 GeV) in their invariant mass axes, M . We have taken $m_\phi = m_\psi = 0.1$ GeV for making a comparative analysis. Thermal widths Γ_ϕ and Γ_ψ for ϕ and ψ , respectively, are basically the contributions at their corresponding pole positions ($M = m_\phi$ and m_ψ), which are marked by dotted line in the left panel of Fig. (6). The Γ_ϕ and Γ_ψ increase with increasing temperature (T) and decreasing three-momentum (\vec{k}). These are shown in the right panel of Fig. (6) and left panel of Fig. (7) respectively. We have presented the normalized values, $m_\phi^2 \Gamma_\phi / g^2$ and Γ_ψ / G^2 to make our descriptions more general for any arbitrary value of coupling constant, g or G . Now, using these thermal widths $\Gamma_\phi(\vec{k}, T)$ and $\Gamma_\psi(\vec{k}, T)$ in Eqs. (30) and (31), we get the shear viscosity coefficients η_ϕ and η_ψ respectively. Their corresponding temperature dependence are shown in upper and lower panels of Fig. (7) on the right side. Here we have again normalized our results for unit coupling constants and so $g^2 \eta_\phi / m_\phi^2$ vs T (upper panel) and $G^2 \eta_\psi$ vs T (lower panel) have been represented in this graph. In Sec.(4), we have pointed out the possibility of infinite number of ladder-type diagrams (shown in Fig. 3) which are supposed to be of same order of magnitude ($\mathcal{O}(1/g^2)$) like the one-loop (shown in Fig. 1) contributions. This is very well known complexity for the calculation of transport coefficient via Kubo approach. A two loop calculation for boson self-energy is derived to check its numerical strength with respect to the one-loop contribution. In the expression for the two-loop, a quantity $F(k, T)$ in the Eq. (74) is

recognized as the main factor to differentiate between the two-loop and the one-loop expression. The contributions of $F^{AB}(\vec{k}, T)$, $F^{CD}(\vec{k}, T)$ and their total $F(\vec{k}, T)$ from Eq. (75) are shown in the lower panel of the left and right side of Fig. (8). The $F^{CD}(\vec{k}, T)$ is numerically so stronger than $F^{AB}(\vec{k}, T)$ that one can confidently assume $F(\vec{k}, T) \simeq F^{CD}(\vec{k}, T)$. The T and \vec{k} dependence of $F(\vec{k}, T)$ are shown in the upper panel of left and right side of Fig. (8) for two different values of fixed \vec{k} and T respectively. Using the $F(\vec{k}, T)$ in Eq. (74) we have obtained the normalized values of $\eta^{(2)}$ (i.e. $\eta^{(2)}g^2/m_\phi^2$) which are displayed by dashed line in the lower panel of Fig. (9). The ratio $\eta^{(2)}/\eta^{(1)}$ vs T is presented in the upper panel of Fig. (9). The figure shows that $\eta^{(2)}$ is substantially suppressed from the one-loop contribution $\eta^{(1)}$. During extension from one-loop to two-loop calculation, the additional thermal distribution functions are introduced in multiplicative way. This may be the main reason of the suppression of $\eta^{(2)}$ from $\eta^{(1)}$. This two loop result is indicating that as the number of loops will be increased, its numerical strength will be successively suppressed. So the one-loop contribution of the shear viscosity for this simple $\phi\phi\Phi$ interaction may be considered as a leading contribution. This approximation is valid especially for the temperature greater than the mass of constituent particles of the medium (i.e. $T > m_\phi$). In some sense this estimation is very general as it is independent of coupling constant g .

6 Summary and conclusion

Taking a special and simple $\phi\phi\Phi$ or $\psi\psi\Phi$ interaction Lagrangian, a diagrammatic analysis of Kubo-type shear viscosity has been presented in this manuscript. At first the simplest possible skeleton, one-loop diagram for ϕ boson (or ψ boson) is evaluated in real-time thermal field theory, where the effective propagators with finite thermal width are used in the $\phi\phi$ or $\psi\psi$ loop. The thermal width of ϕ is extracted from the imaginary part of its thermal self-energy for $\phi\Phi$ or $\psi\Phi$ loop. After the one-loop analysis, the higher order loop diagrams with same power of coupling constant as in the one-loop are inspected. Instead of re-summing them, the next possible skeleton, two-loop diagram is explicitly deduced in RTF. Extending the calculations from one-loop to two-loop, the extra thermal distribution function comes automatically into the picture, for which the numerical strength of two-loop is suppressed from one-loop contribution. It is naturally expected that as we increase the number of loops, the suppression will successively grow. On this basis, the one-loop results may be considered as a leading order results for this simple $\phi\phi\Phi$ interaction. As a practical example, if someone is interested to calculate the shear viscosity of hot pionic medium [13] by using the $\pi\pi\sigma$ as well as $\pi\pi\rho$ interaction (effective) Lagrangian, then one-loop estimation is sufficient for numerical purpose. Again, we know that this Kubo-type one-loop expression of shear viscosity in terms of thermal width coincides exactly with the expression from the relaxation time approximation of kinetic theory. Hence, one can get similar results for the $\phi\phi\Phi$ or $\psi\psi\Phi$ interaction following relaxation time approximation also.

Acknowledgments

Author thanks to Prof. Sourav Sarkar and Prof. Angel Gomez Nicola for their useful help and suggestions. Author also thanks to Abhishek Mishra, Sandeep Gautam, Supriya Mondal for their useful suggestions to improve the writings of this article. This work is financed by Fundacao de Amparo a Pesquisa do Estado de Sao Paulo (FAPESP) under Contract No. 2012/16766-0.

A Calculation of $\pi^{\mu\nu}$:

Using the free Lagrangian densities

$$\mathcal{L} = \frac{1}{2}\partial_\mu\phi\partial^\mu\phi - \frac{1}{2}m_\phi^2\phi^2 \quad (78)$$

and

$$\mathcal{L} = \bar{\psi}(i\gamma^\mu\partial_\mu - m_\psi)\psi \quad (79)$$

for ϕ boson and ψ fermion, their energy momentum tensors can respectively be obtained as

$$\begin{aligned} T_{\rho\sigma} &= -g_{\rho\sigma}\mathcal{L} + \frac{\partial\mathcal{L}}{\partial(\partial^\rho\phi)}\partial_\sigma\phi + \frac{\partial\mathcal{L}}{\partial(\partial^\sigma\phi)}\partial_\rho\phi \\ &= -g_{\rho\sigma}\mathcal{L} + \partial_\sigma\phi\partial_\rho\phi \end{aligned} \quad (80)$$

and

$$\begin{aligned} T_{\rho\sigma} &= -g_{\rho\sigma}\mathcal{L} + \frac{\partial\mathcal{L}}{\partial(\partial^\rho\psi)}\partial_\sigma\psi \\ &= -g_{\rho\sigma}\mathcal{L} + i\bar{\psi}\gamma_\rho\partial_\sigma\psi . \end{aligned} \quad (81)$$

Now, the viscous stress tensor is defined as

$$\pi_{\mu\nu} = t_{\mu\nu}^{\rho\sigma}T_{\rho\sigma} , \quad (82)$$

where

$$t_{\mu\nu}^{\rho\sigma} = \Delta_\mu^\rho\Delta_\nu^\sigma - \frac{1}{3}\Delta_{\mu\nu}\Delta^{\rho\sigma} . \quad (83)$$

Using the relation $t_{\mu\nu}^{\rho\sigma}g_{\rho\sigma}\mathcal{L} = 0$, the $\pi^{\mu\nu}$ for ϕ and ψ can respectively be written as

$$\pi_{\mu\nu} = (\Delta_\mu^\rho\Delta_\nu^\sigma - \frac{1}{3}\Delta_{\mu\nu}\Delta^{\rho\sigma}) \left\{ \frac{\partial_\rho\phi\partial_\sigma\phi}{i\bar{\psi}\gamma_\rho\partial_\sigma\psi} \right\} . \quad (84)$$

B Calculation of $N(q, k)$:

Let us write the 11-component of two point function of viscous stress tensor in terms of field operators. For ϕ field it is given by

$$\begin{aligned} \Pi_{11}(q) &= i \int d^4x e^{iqx} \langle T \pi_{\alpha\beta}(x) \pi^{\alpha\beta}(0) \rangle_\beta \\ &= t_{\alpha\beta}^{\rho\sigma} t_{\mu\nu}^{\alpha\beta} i \int d^4x e^{iqx} \langle T \partial_\rho\phi(x) \partial_\sigma\phi(x) \partial^\mu\phi(0) \partial^\nu\phi(0) \rangle_\beta . \end{aligned} \quad (85)$$

With the help of the Wick's contraction technique, we have

$$\begin{aligned} \Pi_{11}(q) &= t_{\alpha\beta}^{\rho\sigma} t_{\mu\nu}^{\alpha\beta} i \int d^4x e^{iqx} [\langle T \partial_\sigma\phi(x) \underbrace{\partial_\rho\phi(x) \partial^\mu\phi(0) \partial^\nu\phi(0)}_{\text{contraction}} \rangle_\beta \\ &\quad + \langle T \partial_\rho\phi(x) \underbrace{\partial_\sigma\phi(x) \partial^\mu\phi(0) \partial^\nu\phi(0)}_{\text{contraction}} \rangle_\beta] \\ &= t_{\alpha\beta}^{\rho\sigma} t_{\mu\nu}^{\alpha\beta} i \int \frac{d^4k}{(2\pi)^4} [N_{\rho\sigma}^{\mu\nu}(q, k) + N_{\rho\sigma}^{\nu\mu}(q, k)] D_{11}(k) D_{11}(p = q - k) \\ &= i \int \frac{d^4k}{(2\pi)^4} N(q, k) D_{11}(k) D_{11}(p = q - k) , \end{aligned} \quad (86)$$

where

$$\begin{aligned} N(q, k) &= t_{\alpha\beta}^{\rho\sigma} t_{\mu\nu}^{\alpha\beta} [N_{\rho\sigma}^{\mu\nu}(q, k) + N_{\rho\sigma}^{\nu\mu}(q, k)] \\ &= t_{\mu\nu}^{\rho\sigma} [N_{\rho\sigma}^{\mu\nu}(q, k) + N_{\rho\sigma}^{\nu\mu}(q, k)] . \end{aligned} \quad (87)$$

From the one-loop self-energy graph of Fig. (1), the $N_{\rho\sigma}^{\mu\nu}$ can be obtained as

$$N_{\rho\sigma}^{\mu\nu} = -k_\rho(q - k)_\sigma k^\mu(q - k)^\nu \quad (88)$$

and so in the comoving frame (i.e. $u = 1, \vec{0}$), we get

$$N(q, k) = -[\vec{k}^2(\vec{q} - \vec{k})^2 + \frac{\{\vec{k} \cdot (\vec{q} - \vec{k})\}^2}{3}] . \quad (89)$$

Similarly for ψ field,

$$\begin{aligned} \Pi_{11}(q) &= t_{\alpha\beta}^{\rho\sigma} t_{\mu\nu}^{\alpha\beta} i \int d^4x e^{iqx} \langle T \bar{\psi}(x) \gamma_\rho \partial_\sigma \psi(x) \overbrace{\psi(0) \gamma^\mu \partial^\nu \psi(0)} \rangle_\beta \\ &= -i \int \frac{d^4k}{(2\pi)^4} N(q, k) D_{11}(k) D_{11}(p = q + k) , \end{aligned} \quad (90)$$

where

$$\begin{aligned} N(q, k) &= t_{\mu\nu}^{\rho\sigma} N_{\rho\sigma}^{\mu\nu}(q, k) \\ &= t_{\mu\nu}^{\rho\sigma} \text{Tr}[\gamma^\mu(q + k)^\nu (\not{q} + \not{k} + m_p) \gamma_\rho k_\sigma (\not{k} + m_k)] . \end{aligned} \quad (91)$$

In the comoving frame the $N(q, k)$ become

$$N(q, k) = \frac{32}{3} \{k_0(q_0 + k_0)\} \{\vec{k} \cdot (\vec{q} + \vec{k})\} - 4[\{\vec{k} \cdot (\vec{q} + \vec{k})\}^2 + \frac{\vec{k}^2(\vec{q} + \vec{k})^2}{3}] . \quad (92)$$

References

- [1] A. Hosoya, M. Sakagami, and M. Takao, Ann. Phys. 154, 229 (1984).
- [2] R. Horsley and W. Schoenmaker, Nucl. Phys. **B 280**, 716 (1987).
- [3] D. Fernandez-Fraile and A. Gomez Nicola, Eur. Phys. J. **C 62**, 37 (2009).
- [4] D. Fernandez-Fraile and A. Gomez Nicola, Eur. Phys. J. **A 31**, 848 (2007).
- [5] D. Fernandez-Fraile and A. Gomez Nicola, Int. J. Mod. Phys. **E 16** (2007) 3010.
- [6] R. Lang, N. Kaiser and W. Weise Eur. Phys. J. **A 48**, 109 (2012).
- [7] R. Lang, W. Weise, arXiv:1311.4628 [hep-ph].
- [8] S. Jeon, Phys. Rev. **D 47**, 4586 (1993); 52, 3591 (1995).
- [9] E. Wang and U. W. Heinz, Phys. Lett. **B 471**, 208 (1999).
- [10] M.E. Carrington, Hou Defu and R. Kobes, Phys. Rev **D 62**, 025010 (2000)
- [11] M.E. Carrington, Hou Defu and R. Kobes, Phys. Lett. **B 523**, 221 (2001).

- [12] M. A. Valle Basagoiti, Phys. Rev. **D 66**, 045005 (2002).
- [13] S. Ghosh, G. Krein, S. Sarkar, arXiv:1401.5392 [nucl-th].
- [14] S. Ghosh, A. Lahiri, S. Majumder, R. Ray, S. K. Ghosh, Phys. Rev. **C 88**, 068201 (2013).
- [15] D. N. Zubarev *Non-equilibrium statistical thermodynamics* (New York, Consultants Bureau, 1974).
- [16] R. Kubo, J. Phys. Soc. Jpn. **12**, 570 (1957).
- [17] P. Romatschke, Int. J. Mod. Phys. **E 19**, 1 (2010).
- [18] T. Hirano, N. van der Kolk, A. Bilandzic, Lect. Notes Phys. **785** (2010) 139.
- [19] H. Matsumoto, Y. Nakano and H. Umezawa, J. Math. Phys. **25**, 3076 (1984).
- [20] L.V. Keldysh, Sov. Phys. JETP **20**, 1018 (1964).
- [21] A. J. Niemi and G. W. Semenoff, Annals of Physics **152**, 105 (1984).
- [22] S. Mallik, S. Sarkar Eur. Phys. J. **C 61** (2009) 489.
- [23] S. Sarkar, Advances in High Energy Physics, **2013**, 627137 (2013).
- [24] S. Ghosh, *Probing spectral properties of hadrons in hot and dense hadronic matter* (Ph.D. Thesis) HBNI (India), 2012, http://www.hbni.ac.in/phdthesis/thesis_june2013/PHYS04200704005_Sabyasachi_Ghosh.pdf
- [25] S. Gavin, Nucl. Phys. **A 435** (1985) 826.
- [26] M. Prakash, M. Prakash, R. Venugopalan, and G. Welke, Phys. Rep. **227**, 321 (1993).
- [27] S. Mitra, S. Ghosh, and S. Sarkar Phys. Rev. **C 85**, 064917 (2012).
- [28] C. Sasaki, K. Redlich, Nucl. Phys. **A 832** (2010) 62.
- [29] R. Baier, B. Pire, D. Schiff Phys. Rev. **D 38**, 9 (1988).